Time Dependent Density Functional Theory for nuclear reactions

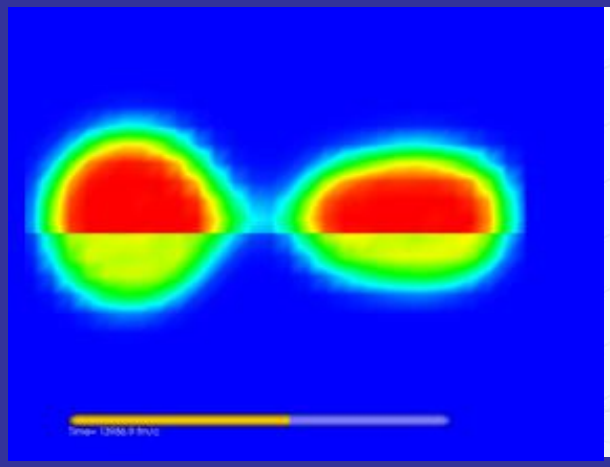

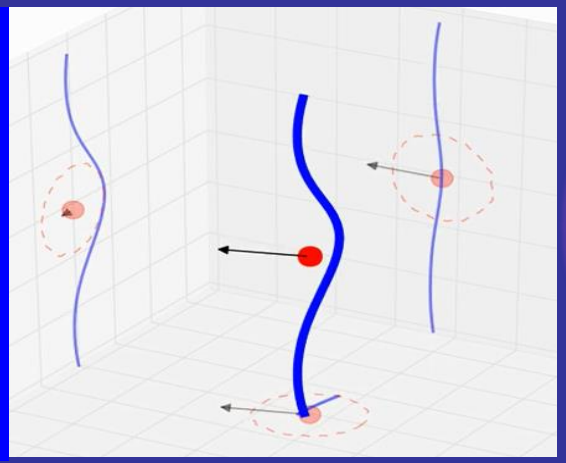

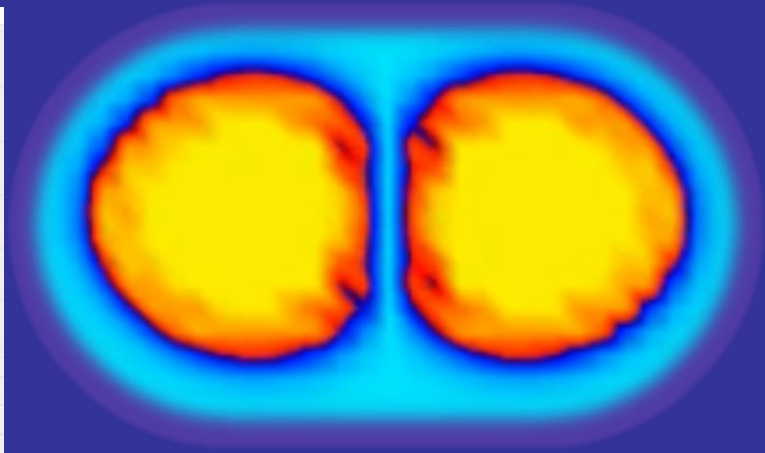

Piotr Magierski (Warsaw University of Technology)

Collaborators:

Warsaw Univ. of Technology

Janina Grineviciute

Kazuyuki Sekizawa (now Niigata U.)

Gabriel Wlazłowski

Konrad Kobuszewski (Ph.D. student)

Bugra Tuzemen (Ph.D. student)

Aurel Bulgac (Univ. of Washington)

Michael M. Forbes (Washington State U.)

Kenneth J. Roche (PNNL)

Ionel Stetcu (LANL)

Shi Jin (Univ. of Washington, Ph.D. student)

GOAL:
Unified description of superfluid dynamics of fermionic systems far from equilibrium based on microscopic theoretical framework.

Microscopic framework = explicit treatment of fermionic degrees of freedom.

Why Time Dependent Density Functional Theory (TDDFT)?

We need to describe the time evolution of (externally perturbed) spatially inhomogeneous, superfluid Fermi system.

Within current computational capabilities TDDFT allows to describe real time dynamics of strongly interacting, superfluid systems of hundred of thousands fermions.

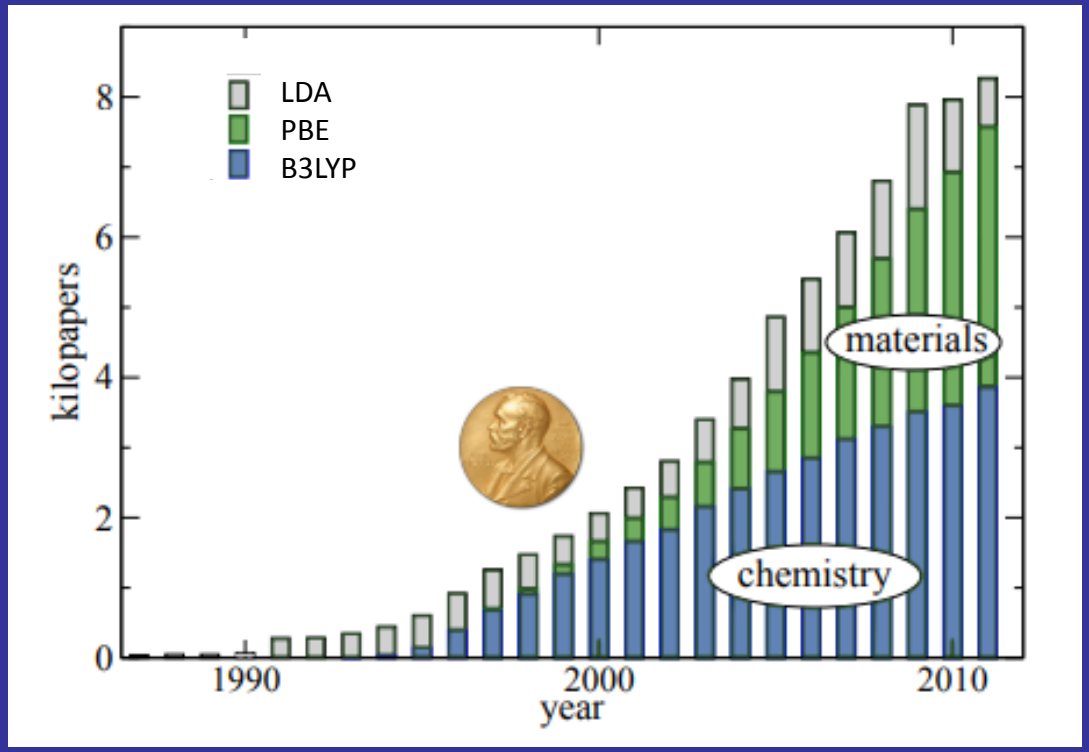

Number of papers using variants of DFT from K.Burke,J.Chem.Phys.136,150901(2012)

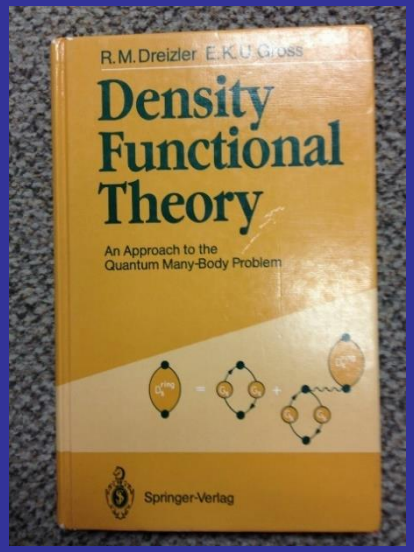

1990

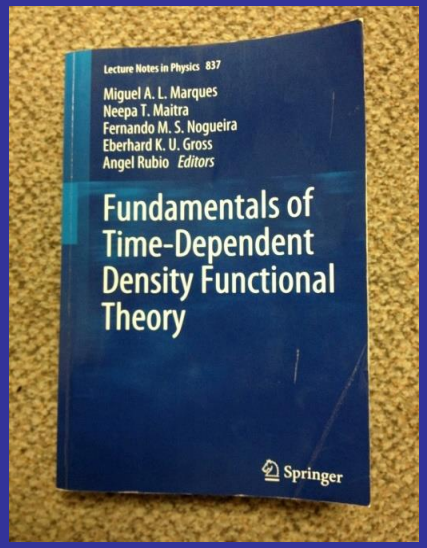

2012

Kohn-Sham scheme

Suppose we are given the density of an interacting system.
There exists a unique noninteracting system with the same density.

Interacting system

$$i\hbar\frac{\partial}{\partial t}\left|\psi(t)\right\rangle = (\hat{T}+\hat{V}(t)+\hat{W})\left|\psi(t)\right\rangle$$

Noninteracting system

$$i\hbar\frac{\partial}{\partial t}\left|\varphi(t)\right\rangle = (\hat{T}+\hat{V}_{KS}(t))\left|\varphi(t)\right\rangle$$

$$\rho(\vec{r},t) = \left\langle\psi(t)\right|\hat{\rho}(\vec{r})\left|\psi(t)\right\rangle = \left\langle\varphi(t)\right|\hat{\rho}(\vec{r})\left|\varphi(t)\right\rangle$$

Hence the DFT approach is essentially exact.

A local extension of DFT to superfluid systems (SLDA) and time-dependent phenomena (TDSLDA) was developed.

Reviews: A. Bulgac, *Time-Dependent Density Functional Theory and Real-Time Dynamics of Fermi Superfluids*, Ann. Rev. Nucl. Part. Sci. 63, 97 (2013); P. Magierski, *Nuclear Reactions and Superfluid Time Dependent Density Functional Theory*, in *"Progress of time-dependent nuclear reaction theory" (Betham Science Publishers 2016)*

Pairing correlations in time-dependent DFT

$$S = \int_{t_0}^{t_1} \left(\left\langle 0(t) \left| i \frac{d}{dt} \right| 0(t) \right\rangle - E[\rho(t), \chi(t)] \right) dt$$

Stationarity requirement produces the set of equations:

$$i\hbar \frac{\partial}{\partial t} \begin{pmatrix} U_\mu(\mathbf{r},t) \\ V_\mu(\mathbf{r},t) \end{pmatrix} = \begin{pmatrix} h(\mathbf{r},t) & \Delta(\mathbf{r},t) \\ \Delta^*(\mathbf{r},t) & -h^*(\mathbf{r},t) \end{pmatrix} \begin{pmatrix} U_\mu(\mathbf{r},t) \\ V_\mu(\mathbf{r},t) \end{pmatrix}$$

$$B(t) = \begin{pmatrix} U(t) & V^*(t) \\ V(t) & U^*(t) \end{pmatrix} = \exp[iG(t)] \qquad G(t) = \begin{pmatrix} h(t) & \Delta(t) \\ \Delta^\dagger(t) & -h^*(t) \end{pmatrix}$$

Orthogonality and completeness has to be fulfilled: $B^\dagger(t)B(t) = B(t)B^\dagger(t) = I$

In order to fulfill the completenes relation of Bogoliubov transform all states need to be evolved!
Otherwise Pauli principle is violated, i.e. the evolved densities do not describe a fermionic system (spurious bosonic effects are introduced).

Consequence: the computational cost increases considerably.

Advantages of TDDFT for nuclear reactions

- The same framework describes various limits: eg. linear and highly nonlinear regimes, adiabatic and nonadiabatic (dynamics far from equilibrium).
- Simulations follow closely the way how experiments are conducted.
- Interaction with basically any external probe (weak or strong) easy to implement.
- TDDFT does not require introduction of hard-to-define collective degrees of freedom and there are no ambiguities arising from defining potential energy surfaces and inertias.
- One-body dissipation, the window and wall dissipation mechanisms are automatically incorporated into the theoretical framework.
- All shapes are allowed and the nucleus chooses dynamically the path in the shape space, the forces acting on nucleons are determined by the nucleon distributions and velocities, and the nuclear system naturally and smoothly evolves into separated fission fragments.
- There is no need to introduce such unnatural quantum mechanical concepts as "rupture" and there is no worry about how to define the scission configuration.

Areas of applications

$\frac{\Delta}{\varepsilon_F} \le 0.5$

$\frac{\Delta}{\varepsilon_F} \le 0.03$

$\frac{\Delta}{\varepsilon_F} \le 0.1-0.2$

Ultracold atomic (fermionic) gases. Unitary regime.

Dynamics of quantum vortices, solitonic excitations, quantum turbulence.

Astrophysical applications.

Modelling of neutron star interior (glitches): vortex dynamics, dynamics of inhomogeneous nuclear matter (in strong magnetic fields).

Nuclear physics.

Induced nuclear fission, fusion, collisions.

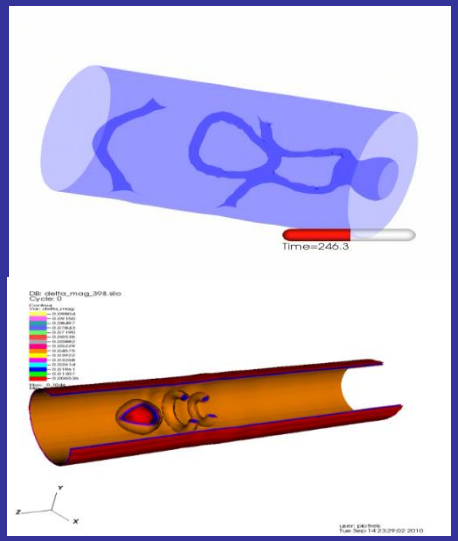

Phys. Rev. Lett. 120, 253002 (2018)
Phys. Rev. Lett. 112, 025301 (2014)
Science **332**, 1288 (2011).

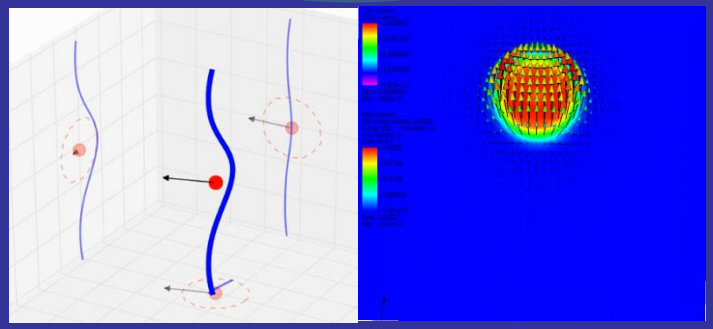

Phys. Rev. Lett. **117**, 232701 (2016)
Phys. Rev. Lett. 110, 241102 (2013)

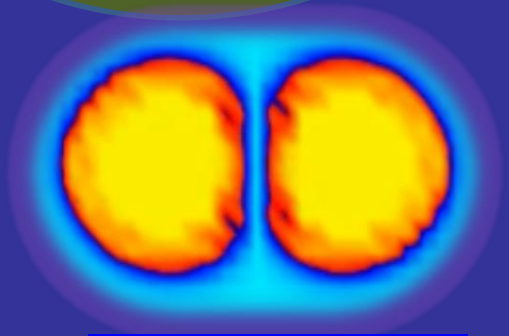

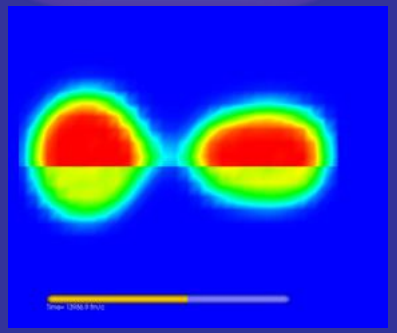

Phys. Rev. Lett. **119**, 042501 (2017)
Phys. Rev. Lett. **116**, 122504 (2016)
Phys. Rev. Lett. **114**, 012701 (2015)

Examples of applications:

- *Collisions of medium or heavy superfluid nuclei*
- *Nuclear induced fission*

Nuclear collisions

Collisions of superfluid nuclei having different phases of the pairing fields

Motivated by experiments on ultracold atomic gases: merging two 6Li clouds

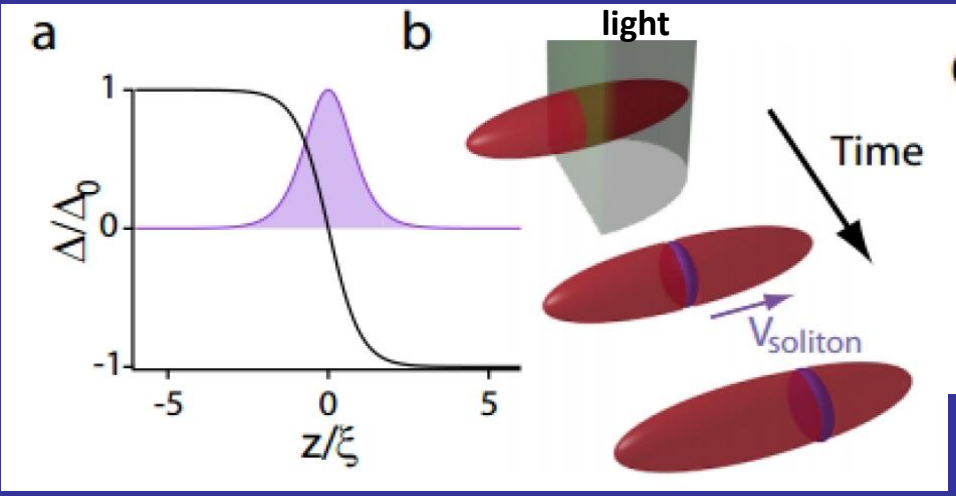

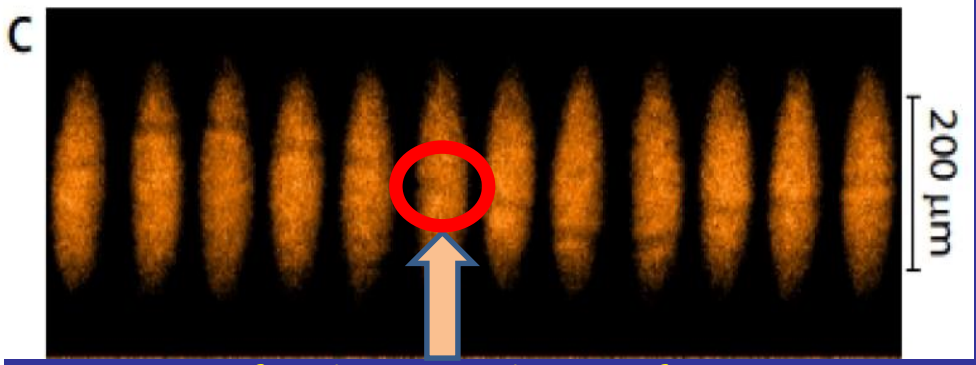

Creation of a „**heavy soliton**" after merging two superfluid atomic clouds.
T. Yefsah et al., Nature 499, 426 (2013).

Sequence of decays of topological excitations is reproduced by TDSLDA:
Wlazłowski, et al.,Phys. Rev. A91, 031602 (2015)

In the context of nuclear systems the main questions are:

-how a possible solitonic structure can be manifested in nuclear system?

-what observable effect it may have on heavy ion reaction:
kinetic energies of fragments, capture cross section, etc.?

Clearly, we cannot control phases of the pairing field in nuclear experiments and the possible signal need to be extracted after averaging over the phase difference.

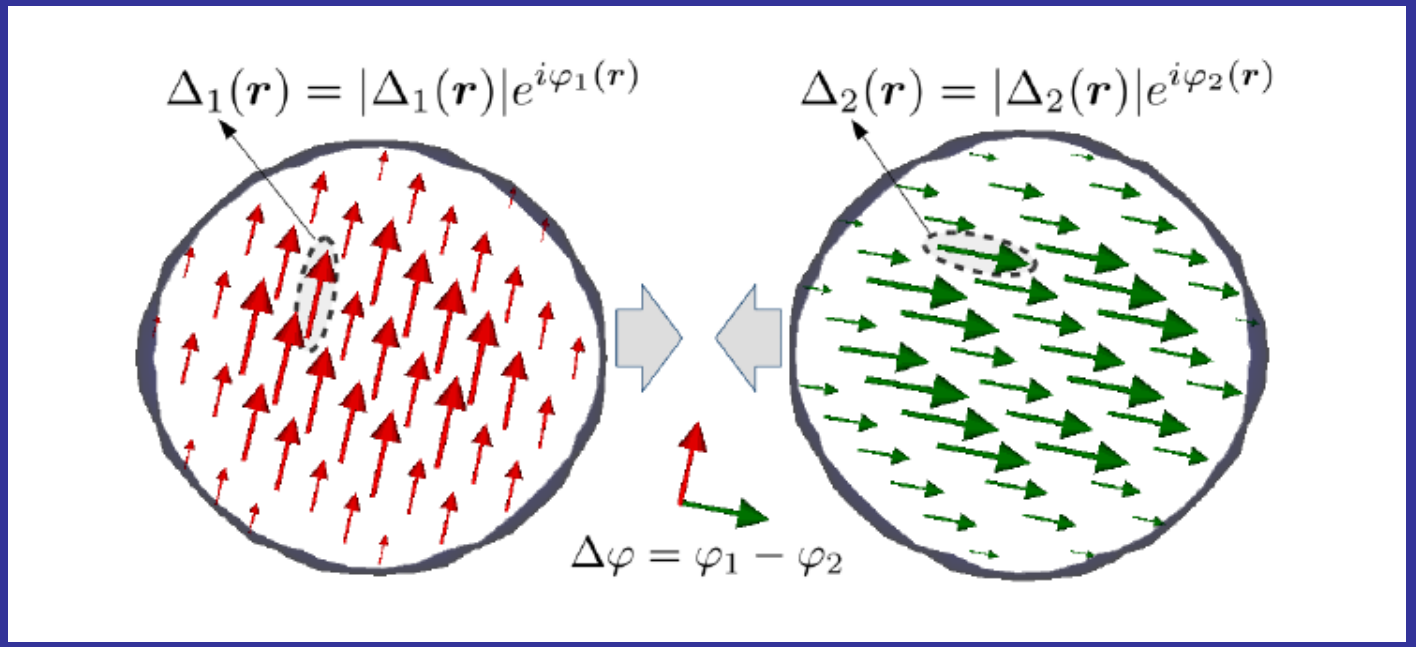
$\Delta_1(\boldsymbol{r}) = |\Delta_1(\boldsymbol{r})|e^{i\varphi_1(\boldsymbol{r})}$
$\Delta_2(\boldsymbol{r}) = |\Delta_2(\boldsymbol{r})|e^{i\varphi_2(\boldsymbol{r})}$
$\Delta\varphi = \varphi_1 - \varphi_2$

Ultracold atomic gases: two regimes for realization of the Josephson junction

Weak coupling (weak link)

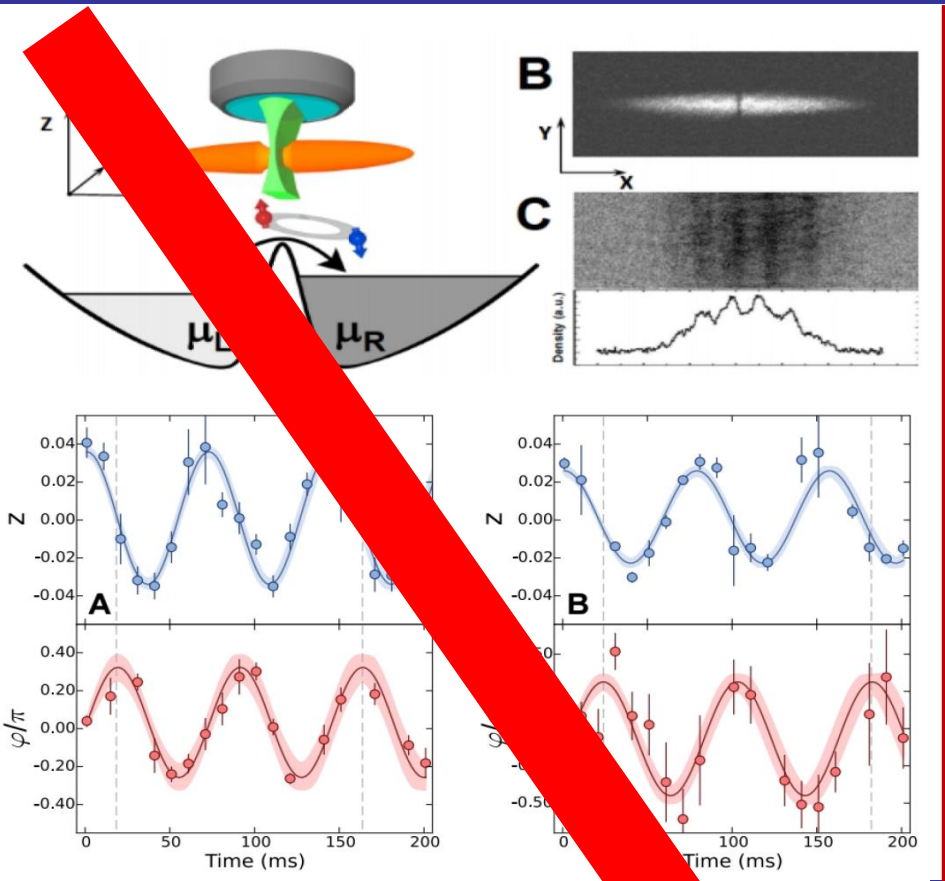

Observation of ***AC Josephs effect*** between two 6Li atomic cloud

It need not to be accompanied creation of a topological excitati

G. Valtolina et al., Science 350, 1505 (2015

Strong coupling

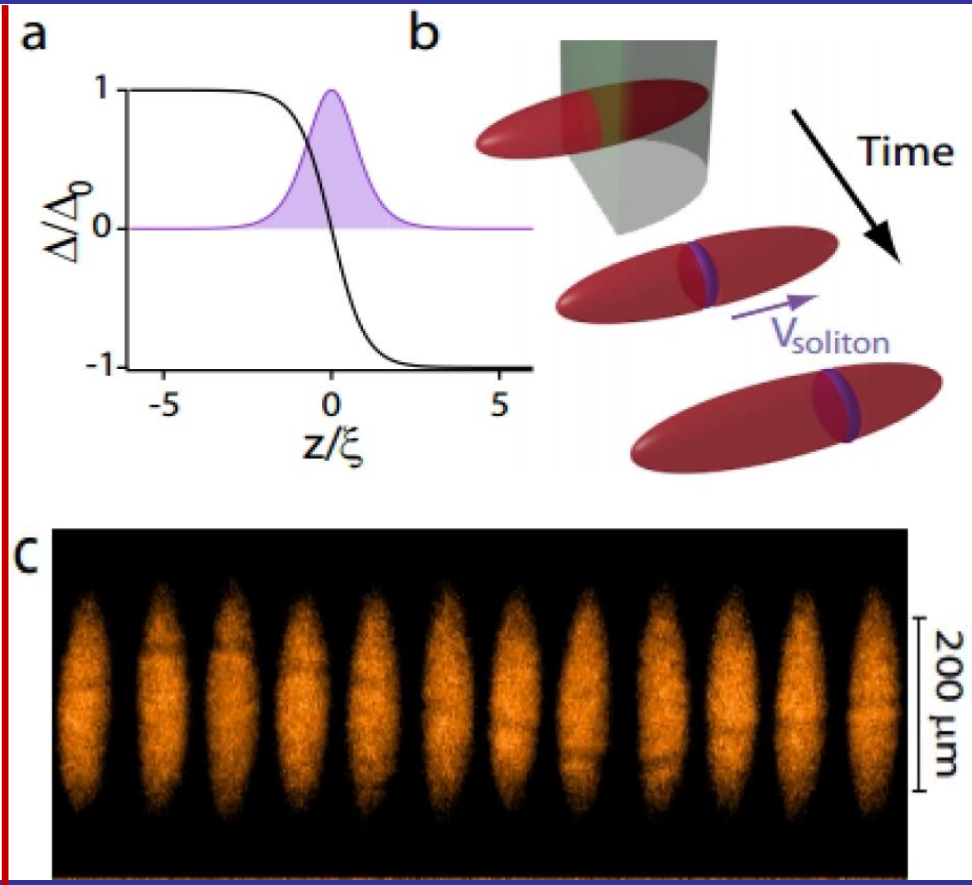

Creation of a „heavy soliton" after merging two superfluid atomic clouds.

T. Yefsah et al., Nature 499, 426 (2013).

Estimates for the magnitude of the effect

At first one may think that the magnitude of the effect is determined by the nuclear pairing energy which is of the order of MeV's in atomic nuclei (according to the expression):

$$\frac{1}{2} g(\varepsilon_F)\left|\Delta\right|^2; \quad g(\varepsilon_F) \text{ - density of states}$$

On the other hand the energy stored in the junction can be estimated from Ginzburg-Landau (G-L) approach:

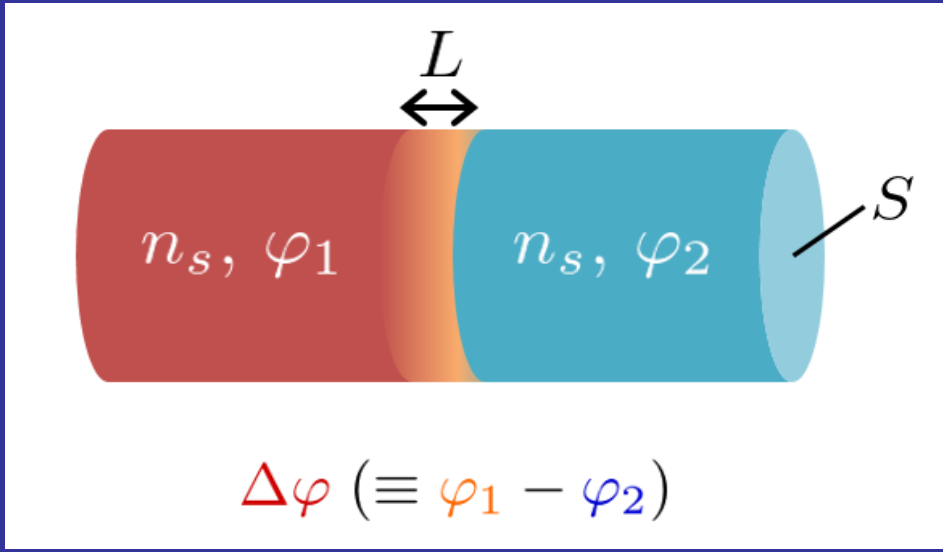

$$E_j = \frac{S}{L}\frac{\hbar^2}{2m} n_s \sin^2\frac{\Delta\varphi}{2}$$

For typical values characteristic for two medium nuclei: $E_j \approx 30 MeV$

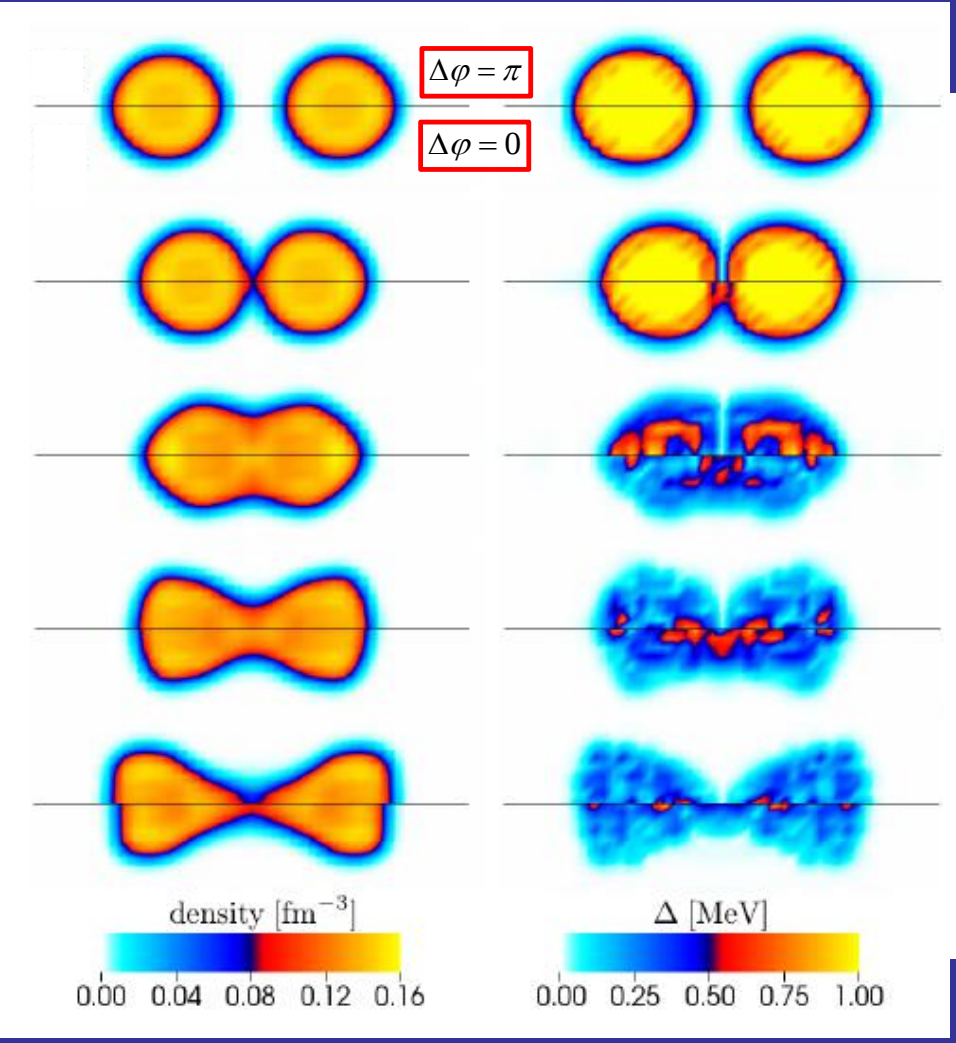

Total kinetic energy of the fragments (TKE)

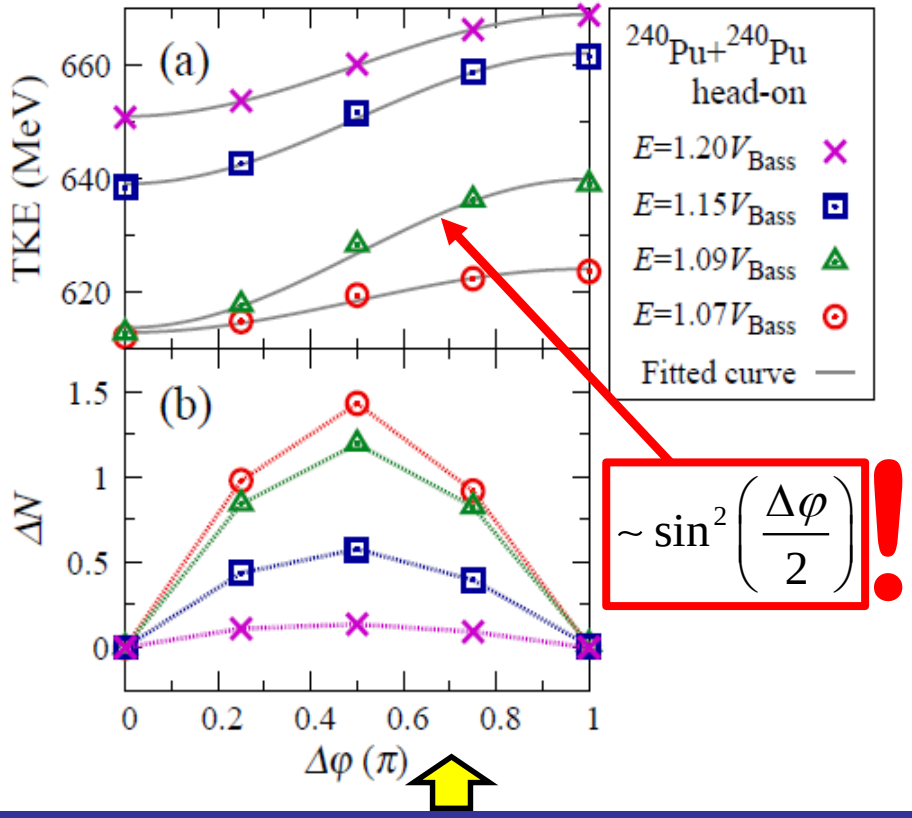

Average particle transfer between fragments.

Creation of the solitonic structure between colliding nuclei prevents energy transfer to internal degrees of freedom and consequently enhances the kinetic energy of outgoing fragments.
Surprisingly, the gauge angle dependence from the G-L approach is perfectly well reproduced in the kinetic energies of outgoing fragments!

$^{90}Zr + {}^{90}\mathrm{Zr}$ at energy $E \simeq V_{Bass}$

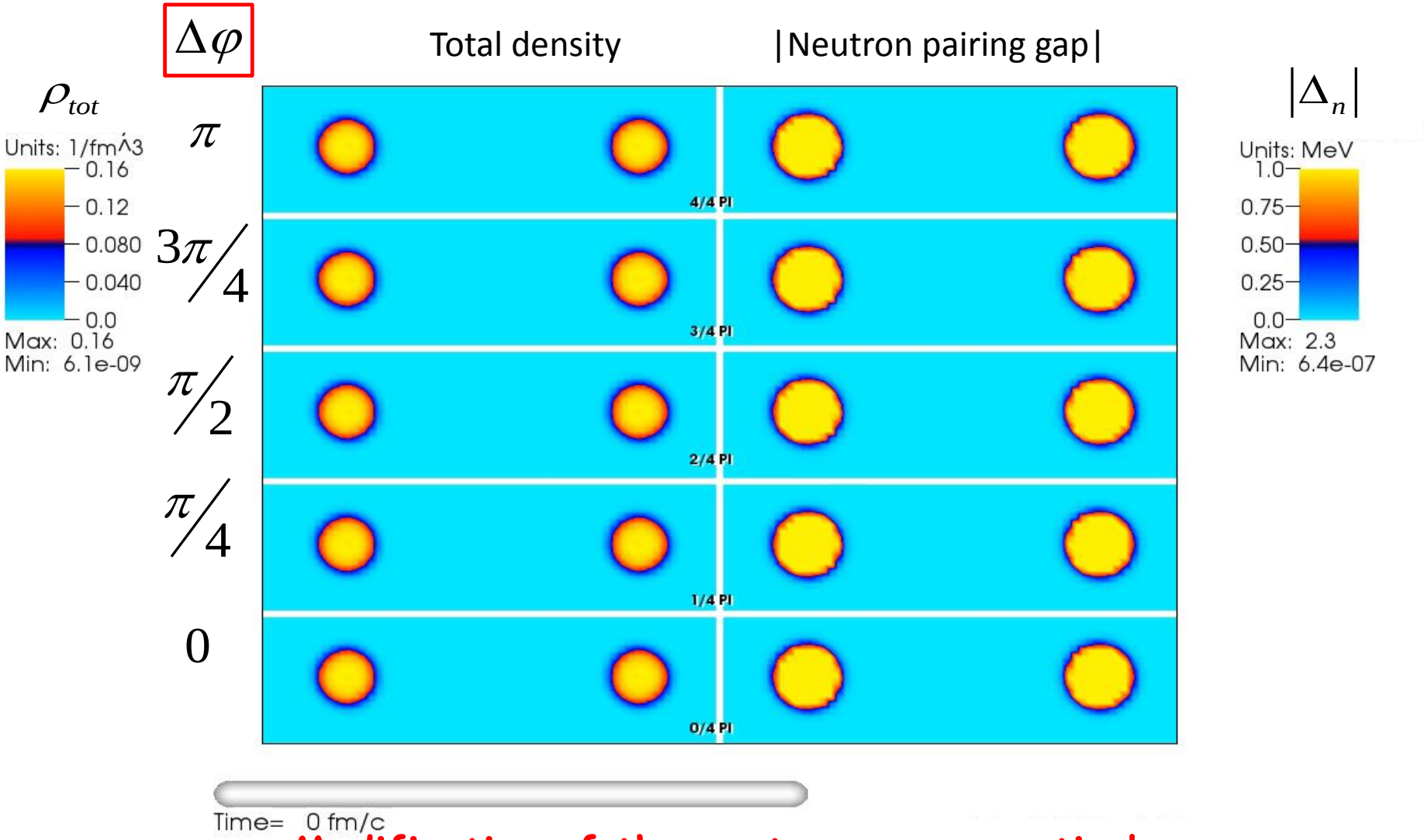

Modification of the capture cross section!

P. Magierski, K. Sekizawa, G. Wlazłowski, Phys. Rev. Lett. 119 042501 (2017)

See also for light nuclei: Y. Hashimoto, G. Scamps, Phys. Rev. C94, 014610 2016)

Effective barrier height for fusion as a function of the phase difference

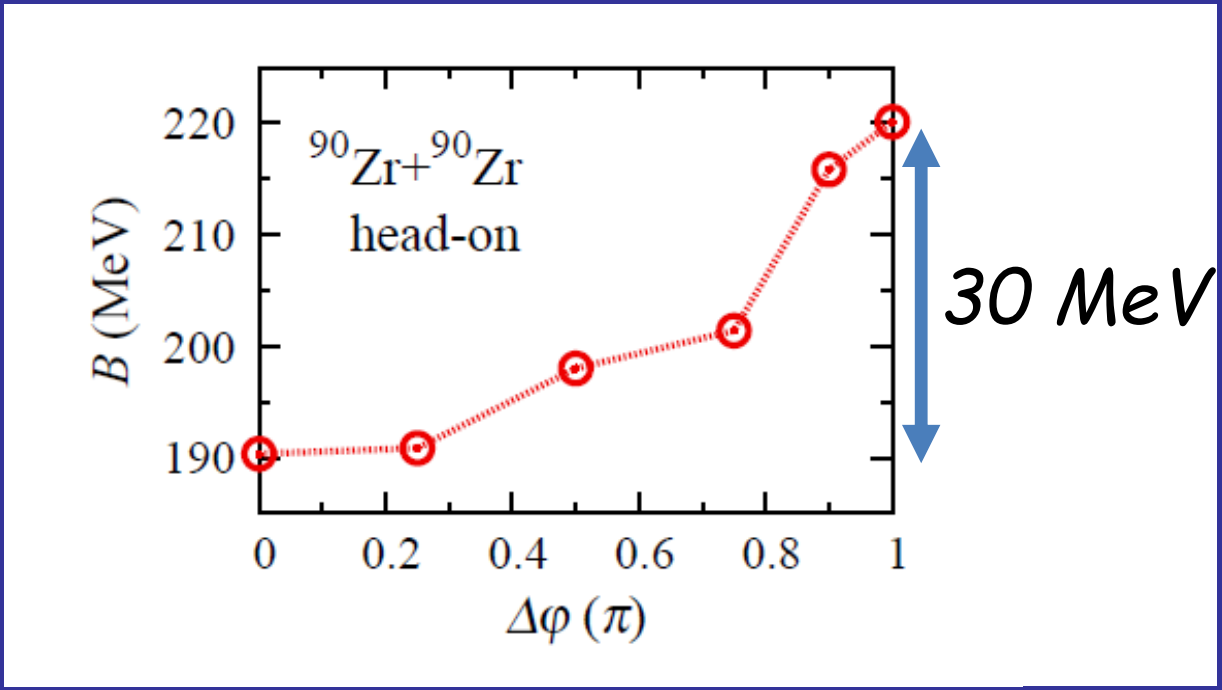

What is an average extra energy needed for the capture?

$$E_{extra} = \frac{1}{\pi}\int_0^{\pi}\left(B(\Delta\varphi) - V_{Bass}\right)d(\Delta\varphi) \approx 10MeV$$

The phase difference of the pairing fields of colliding medium or heavy nuclei produces a similar solitonic structure as the system of two merging atomic clouds.
The energy stored in the created junction is subsequently released giving rise to an increased kinetic energy of the fragments. The effect is found to be of the order of 30MeV for medium nuclei and occur for energies up to 20-30% of the barrier height.

P. Magierski, K. Sekizawa, G. Wlazłowski, Phys. Rev. Lett. 119 042501 (2017)

Fission dynamics of ^{240}Pu

Initial configuration of ^{240}Pu is prepared at the barrier (saddle point) at quadrupole Deformation *Q=165b* and excitation energy *E=8.08 MeV*:

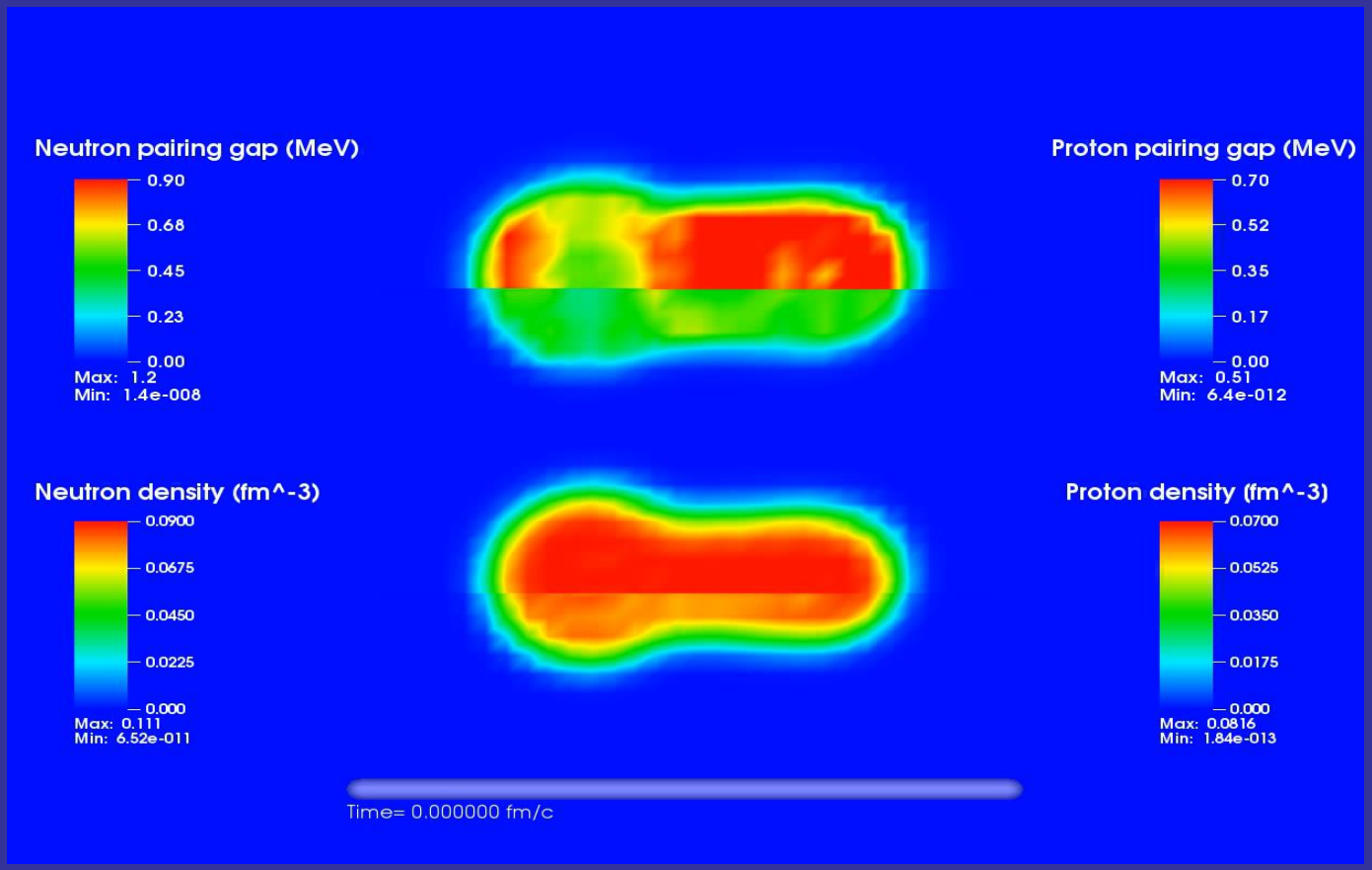

During the process shown, the exchange of about 2 neutrons and 3 protons occur between fragments before the actual fission occurs.

Interestingly the fragment masses seem to be relatively stiff with respect to changes of the initial conditions.

The saddle-scission time is considerably longer than in simplified approaches.

A. Bulgac, P.Magierski, K.J. Roche, and I. Stetcu, Phys. Rev. Lett. 116, 122504 (2016)

Fission dynamics of ^{240}Pu

A typical trajectory of fissioning ^{240}Pu in the collective space at excitation excitation energy of *E=8-9 MeV*:

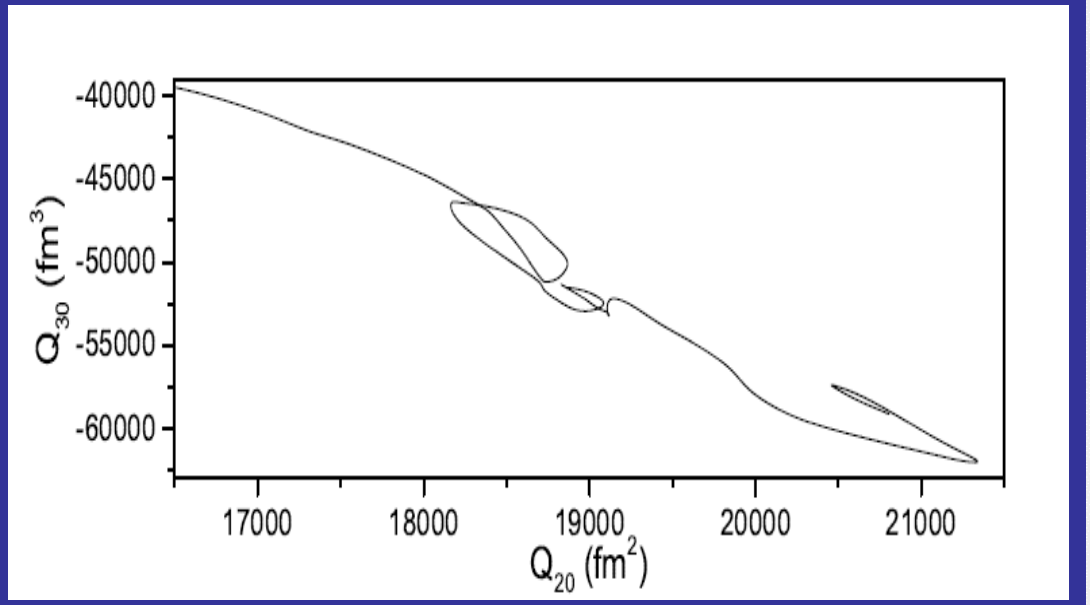

J. Grinevicute, P. Magierski, et al (in preparation).

Accelerations in quadrupole and octupole moments along the fission path

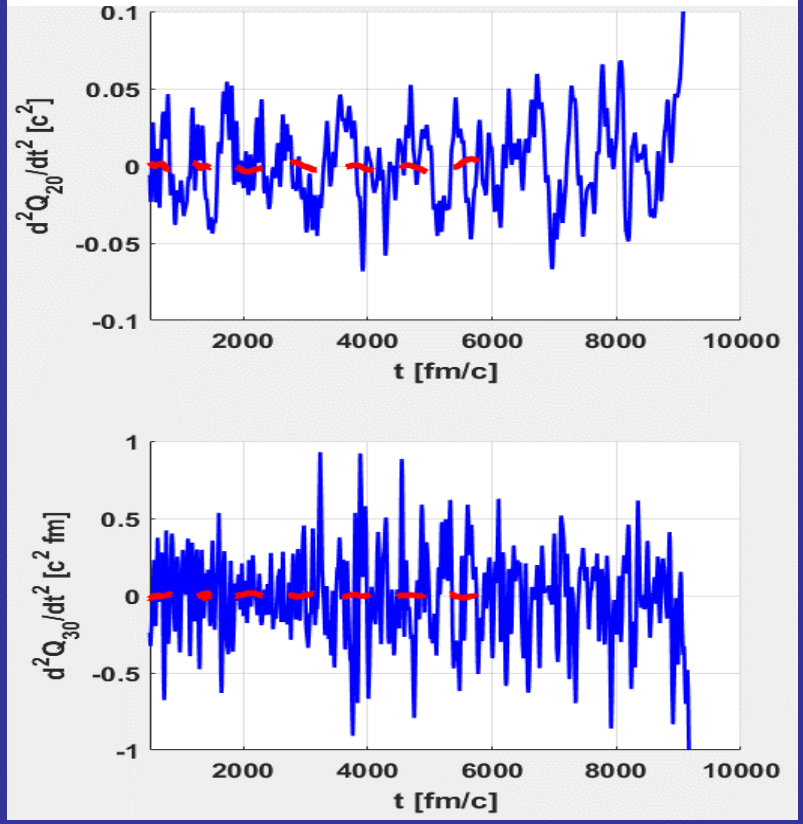

Note that despite the fact that nucleus is already beyond the saddle point the collective motion on the time scale of 1000 fm/c and larger is characterized by the constant velocity (*see red dashed line for an average acceleration*) till the very last moment before splitting. On times scales, of the order of 300 fm/c and shorter, the collective motion is a subject to random-like kicks indicating strong coupling to internal d.o.f

TDSLDA trajectories on the collective potential surface originating from various initial configurations

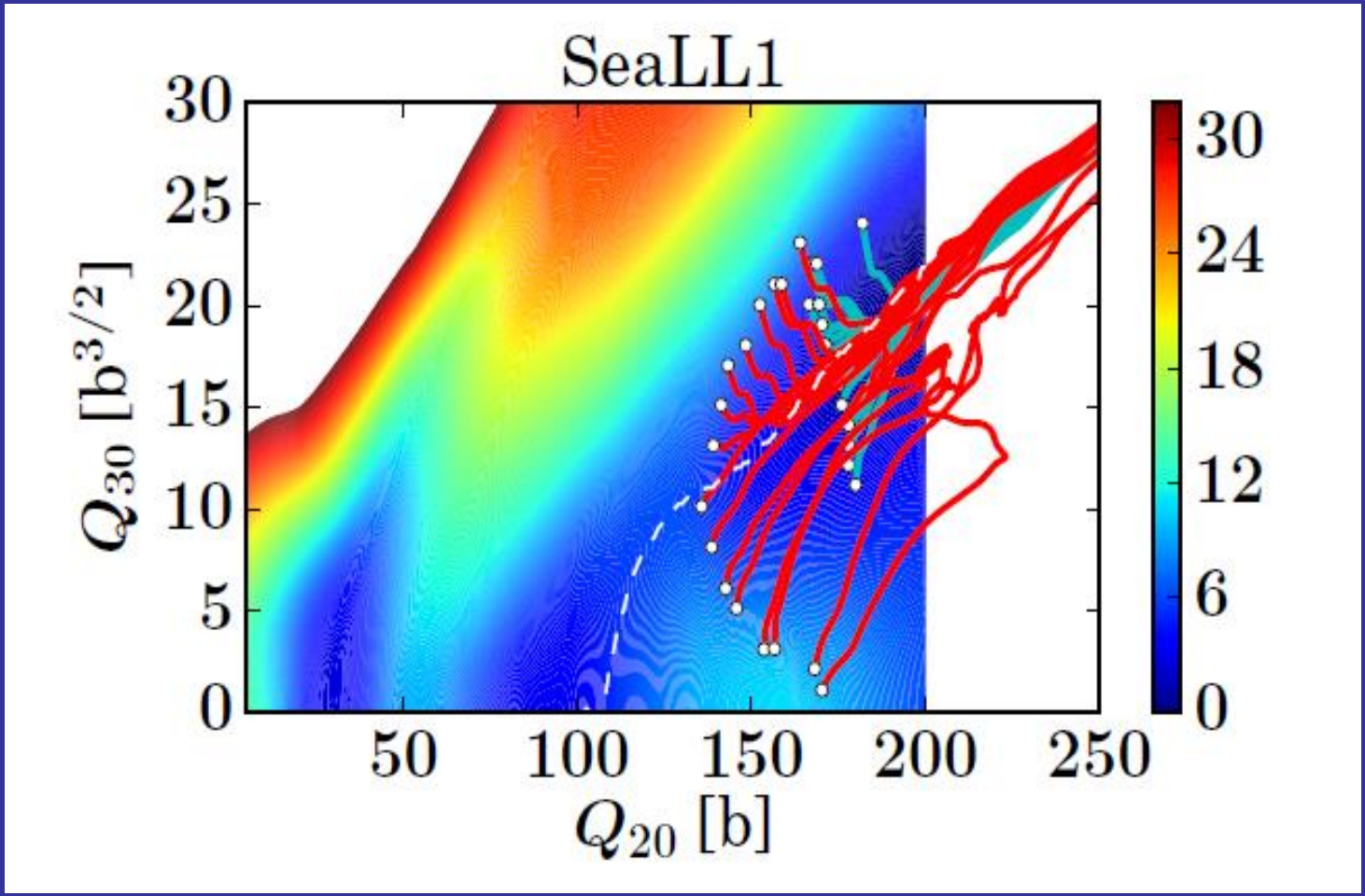

A. Bulgac, et al., arXive: 1806.00694

The final scission configuration is relatively independent on the initial condition (providing it starts at or beyond the saddle point).
One needs a kind of stochastic extension to account for fluctuations.

Nuclear induced fission dynamics:

It is important to realize that these results indicate that the motion is not adiabatic, although it is slow.

Although the average collective velocity is constant till the very last moment before scission, the system heats up as the energy flows irreversibly from collective to intrinsic degrees of freedom.

This may create problems for approaches based on ATDHF(B) or TDGCM as no irreversible energy transfer between collective and Intrinsic is possible there.

Remarks on the fragment kinetic and excitation energy sharing within the TDDFT

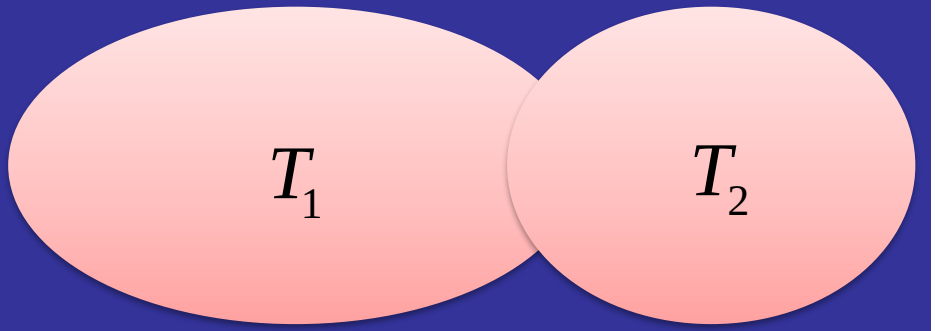

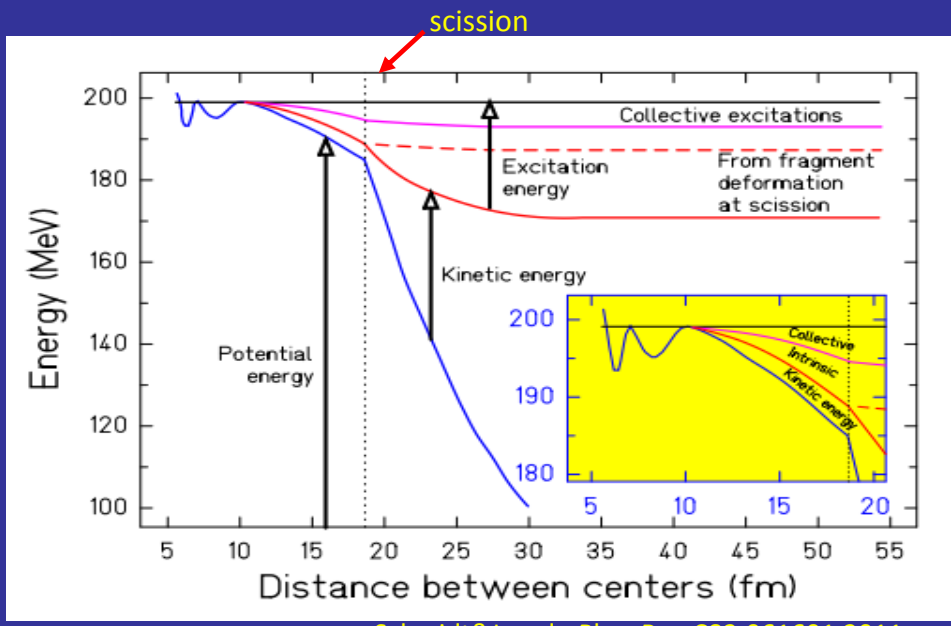

Schmidt&Jurado:Phys.Rev.C83:061601,2011

In the to-date approaches it is usually assumed that the excitation energy has 3 components (Schmidt&Jurado:Phys.Rev.C83:061601,2011 Phys.Rev.C83:014607,2011):

- deformation energy
- collective energy (energy stored in collective modes)
- intrinsic energy (specified by the temperature)

It is also assumed that the intrinsic part of the energy is sorted according to the total entropy maximization of two nascent fragments (i.e. according to temperatures, level densities) and the fission dynamics does not matter.

In TDDFT such a decomposition can be performed as well.
The intrinsic energy in TDDFT will be partitioned dynamically (no sufficient time for equilibration).

Induced fission of 240Pu

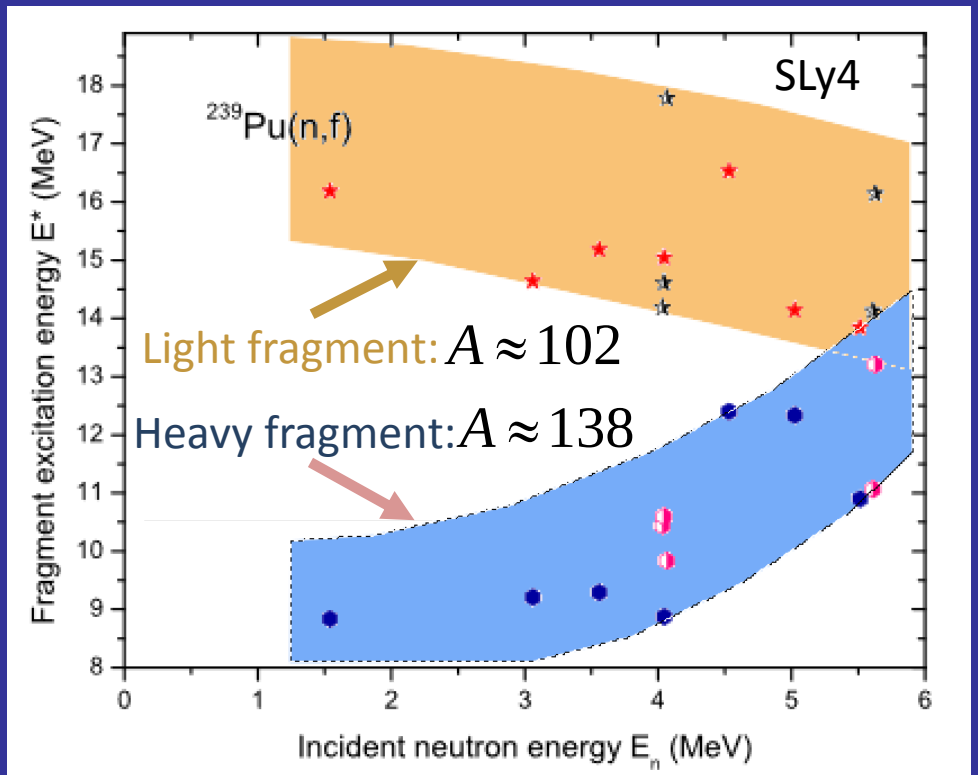

E^* (MeV)	E_n (MeV)	TKE_{TDSLDA} (MeV)	TKE_{syst} (MeV)	err (%)	Z_L	N_L
8.08	1.542	173.81	177.26	1.95	40.825	62.246
9.60	3.063	174.73	176.73	1.13	40.500	61.536
10.10	3.560	179.09	176.56	1.43	41.625	62.783
10.57	4.032	173.67	176.39	1.55	40.092	61.256
10.58	4.043	173.39	176.39	1.70	40.146	61.388
10.58	4.047	175.11	176.39	0.72	40.313	61.475
10.60	4.065	174.75	176.38	0.92	40.904	62.611
11.07	4.534	176.46	176.22	0.14	41.495	63.134
11.56	5.024	175.15	176.05	0.51	40.565	61.894
12.05	5.515	176.75	175.88	0.49	40.412	61.809
12.15	5.610	176.36	175.84	0.29	40.355	61.695
12.16	5.626	176.10	175.84	0.15	41.386	62.764

The lighter fragment is more excited (and strongly deformed) than the heavier one.

Excitation energies are not shared proportionally to mass numbers of the fragments!

$$\mathrm{TKE} = 177.80 - 0.3489 E_n \quad [\text{in MeV}],$$

Nuclear data evaluation, Madland (2006)

Calculated TKEs slightly reproduce experimental data with accuracy < 2%

J. Grineviciute, et al. (in preparation)

see also:

A. Bulgac, P. Magierski, K.J. Roche, and I. Stetcu, Phys. Rev. Lett. 116, 122504 (2016)

Decomposition of the excitation energy into collective and noncollective part

Total excitation energy of the fragments

Intrinsic excitation energy of the fragments:

$$E_{exc.}^{\text{int}} = E_{exc.}^{tot} - \bar{E}_{Thomas-Fermi}$$

$$\bar{E}_{Thomas-Fermi} = \frac{1}{\Delta T}\int_{T_{scission}}^{T_{scission}+\Delta T} E_{Thomas-Fermi}(t)dt$$

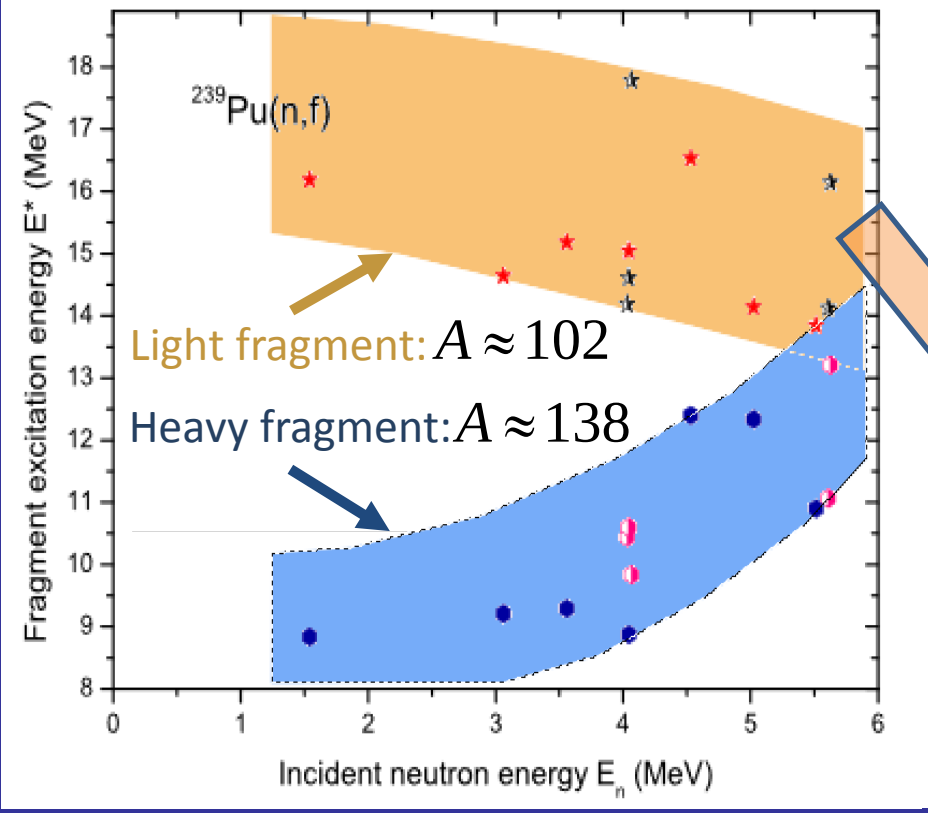

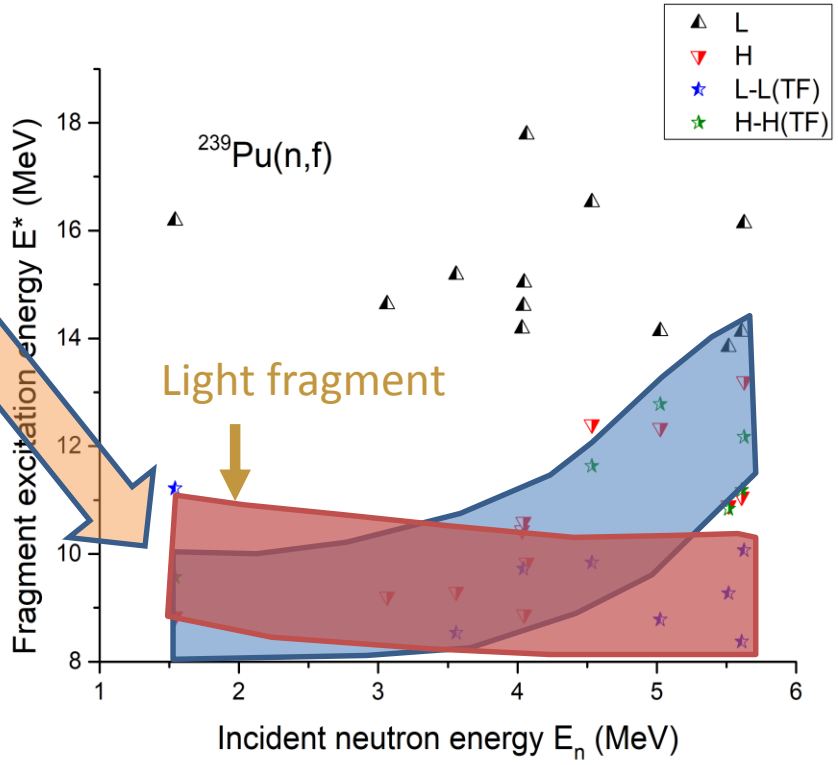

J. Grineviciute, et al. (in preparation)

Energy stored in collective modes: < 2MeV

Summarizing

- TDDFT extended to superfluid systems and based on the local densities offers a flexible tool to study quantum superfluids far from equilibrium.
- TDDFT offers an unprecedented opportunity to test the nuclear energy density functional for large amplitude collective motion, non-equilibrium phenomena.
- For nuclear fission of 240Pu TKEs are reproduced with <2% accuracy for the range of the neutron incident energies: 1.5 - 5.5 MeV.
  TDDFT offers an easy way to extract excitation energy sharing between fragments (experimental data needed!).
- In the context of nuclear reaction extension of TDDFT is needed in order to be able to address the mass and TKE distributions.

- **Future plans:**
- Ultracold atoms: investigation of quantum turbulence in Fermi systems; topological excitations in spin-polarized atomic gases in the presence of LOFF phase.
- Neutron star: Provide a link between large scale models of neutron stars and microscopic studies; towards the first simulation of the glitch phenomenon based on microscopic input.
- Nuclear physics: The dependence of quasifission process on pairing.

Selected supercomputers (CPU+GPU) currently in use:

Piz Daint: 7.787 PFlops
(Swiss National Supercomputing Centre)

HA-PACS: 0.802 PFlops
(University of Tsukuba)

Tsubame: 5.7 PFlops
(Tokyo Institute of Technology)

Titan: 27 PFlops
(ORNL Oak Ridge)

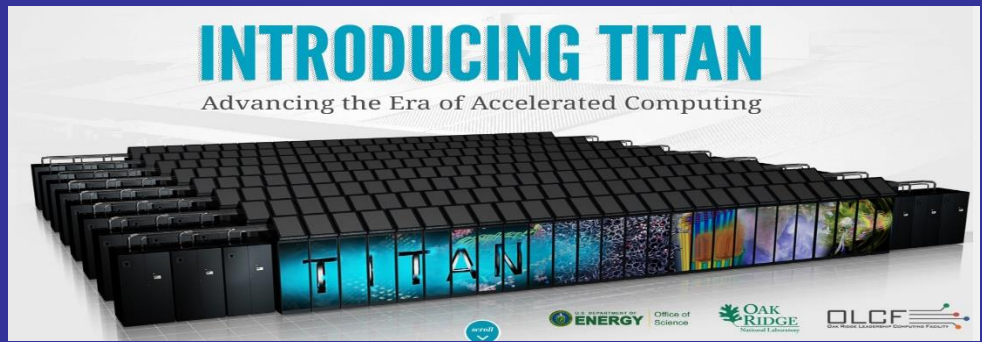

Additional issues related to TDDFT

DFT Basics - ground state

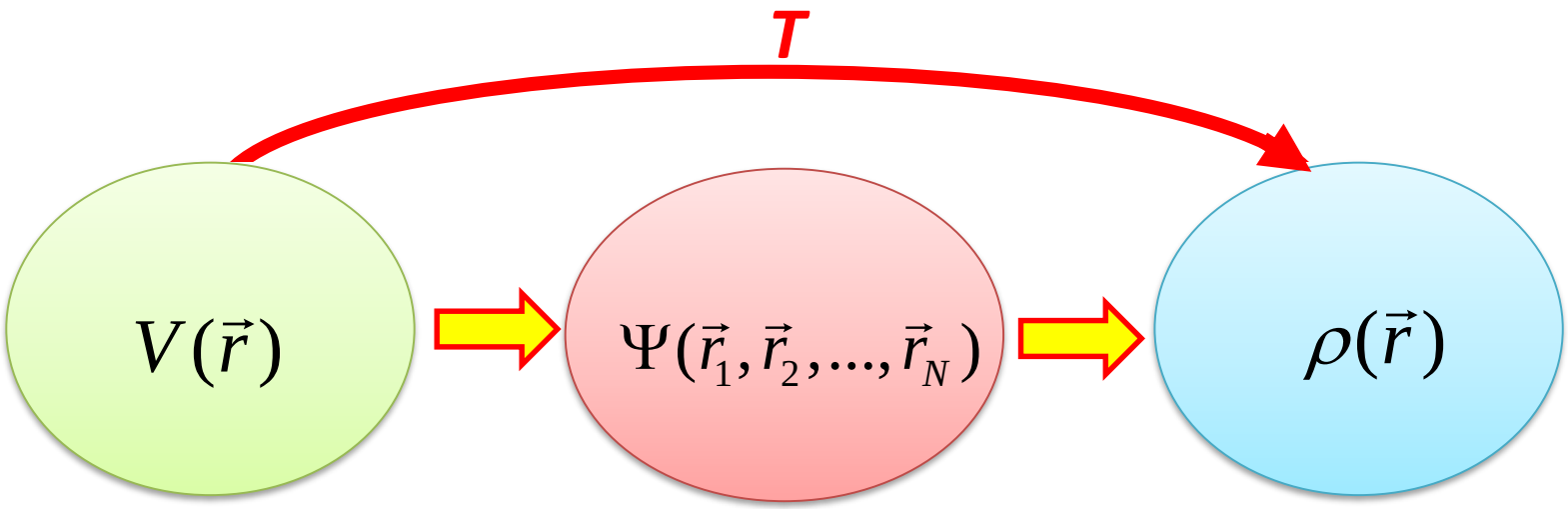

Hohenberg – Kohn theorem (1964):

$T : V(\vec{r}) \rightarrow \rho(\vec{r})$ *is invertible*

Consequences: 1) energy density functional exists:

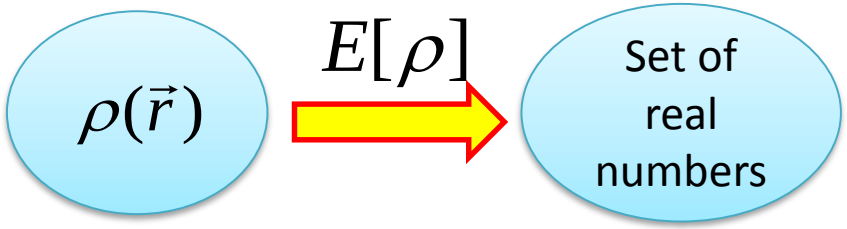

2) every quantum mechanical observable is completely determined by the ground state density: $\Psi(\vec{r}_1,\vec{r}_2,...,\vec{r}_N) = \Psi[\rho](\vec{r}_1,\vec{r}_2,...,\vec{r}_N)$

TDDFT Basics - excited states

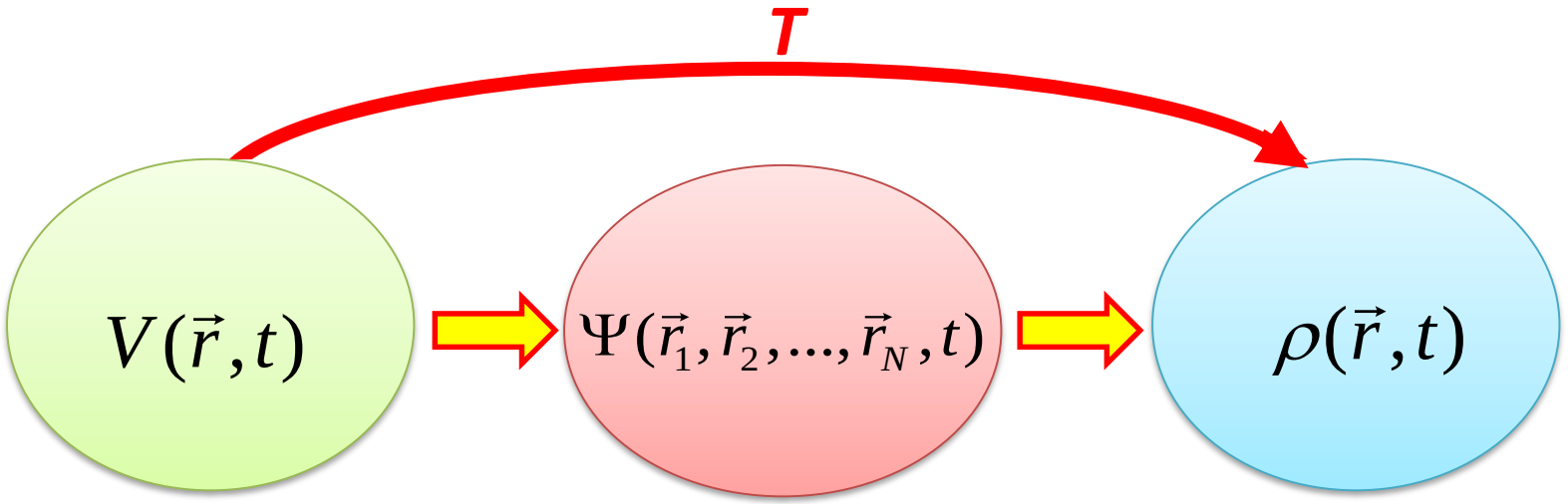

Runge-Gross mapping(1984):

$$i\hbar\frac{\partial}{\partial t}|\psi(t)\rangle = \hat{H}|\psi(t)\rangle, \quad |\psi_0\rangle = |\psi(t_0)\rangle$$

$$\frac{\partial\rho}{\partial t} + \nabla\cdot\vec{j} = 0$$

$$\rho(\vec{r}) \leftrightarrow e^{i\alpha(t)}\Psi[\rho](\vec{r}_1,\vec{r}_2,...,\vec{r}_N)$$

TDDFT variational principle also exists but it is more tricky:

$$F[\psi_0,\rho] = \int_{t_0}^{t_1}\langle\psi[\rho]|\left(i\hbar\frac{\partial}{\partial t} - \hat{H}\right)|\psi[\rho]\rangle\, dt$$

E. Runge, E.K.U Gross, PRL 52, 997 (1984)
B.-X. Xu, A.K. Rajagopal, PRA 31, 2682 (1985)
G. Vignale, PRA77, 062511 (2008)

Pairing as an energy gap

Single-particle levels

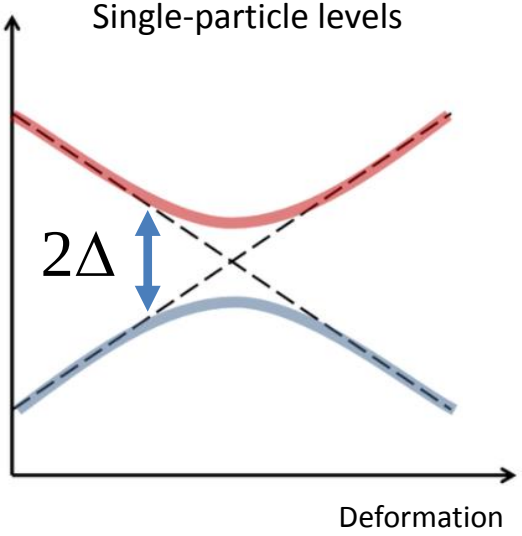

Quasiparticle energy:

$$E_{qp} = \sqrt{(\varepsilon - \mu)^2 + |\Delta|^2}$$

Potential energy surface

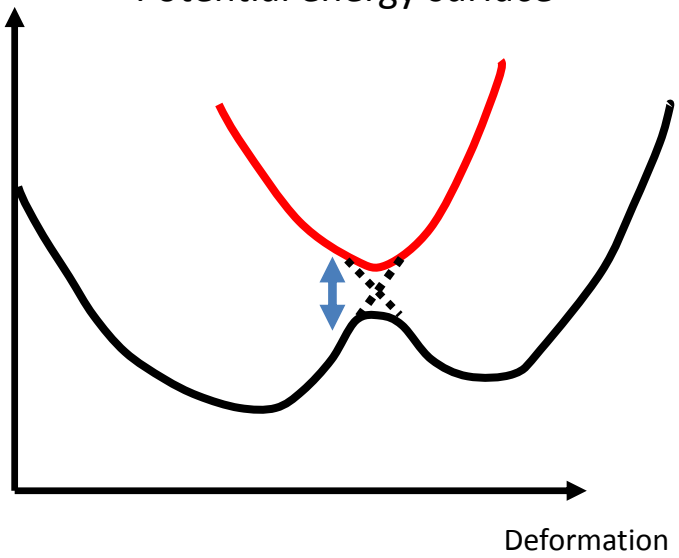

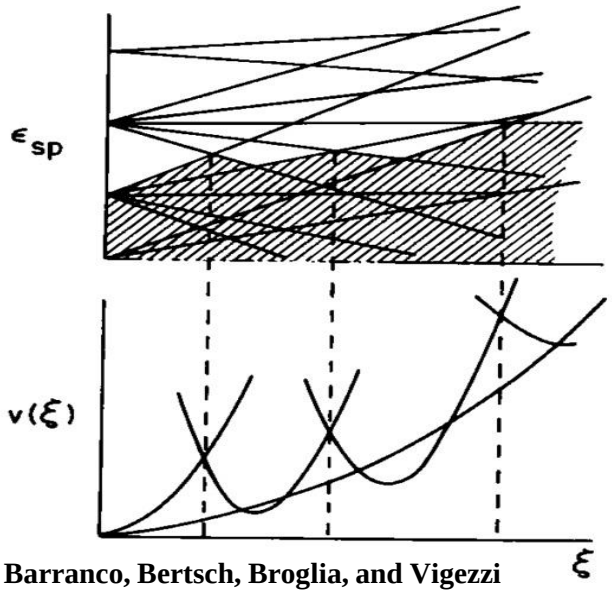

From Barranco, Bertsch, Broglia, and Vigezzi
Nucl. Phys. A512, 253 (1990)

As a consequence of pairing correlations large amplitude nuclear motion becomes more adiabatic.

While a nucleus elongates its Fermi surface becomes oblate and its sphericity must be restored

Hill and Wheeler, PRC, 89, 1102 (1953)
Bertsch, PLB, 95, 157 (1980)

Pairing as a field

$$\Delta(\vec{r},t) = \left|\Delta(\vec{r},t)\right| e^{i\phi(\vec{r},t)}$$

Both magnitude and phase may have a nontrivial spatial and time dependence.

Example of a nontrivial spatial dependence: *quantum vortex*

Vortex structure – section through the vortex core

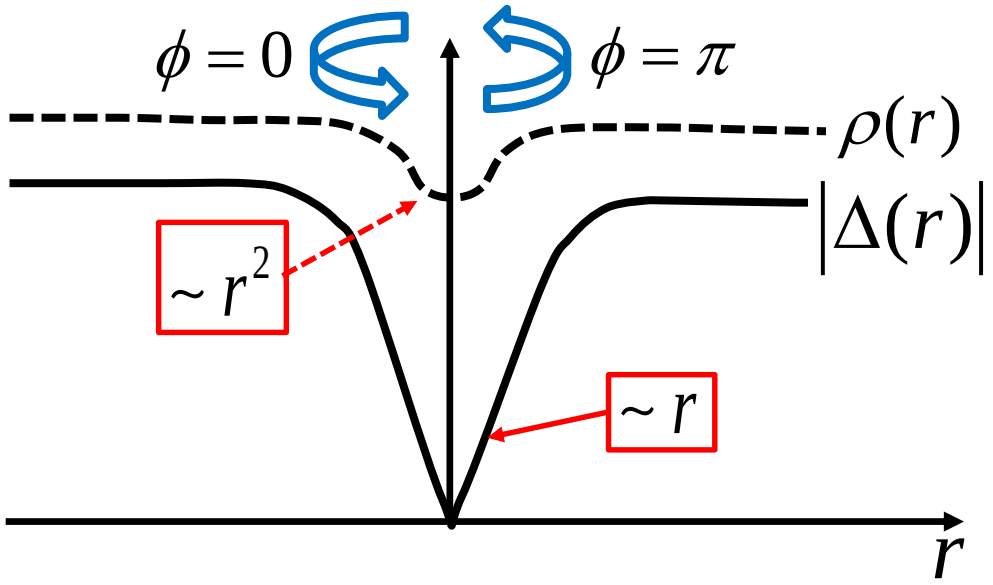

Example of a topological excitation: magnitude of the pairing gap vanishes in the vortex core.

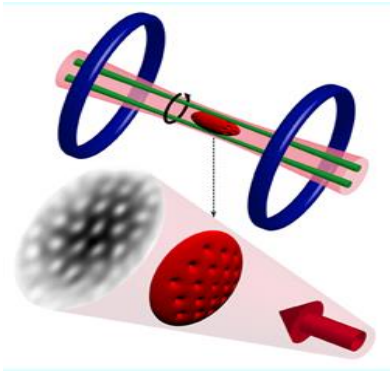

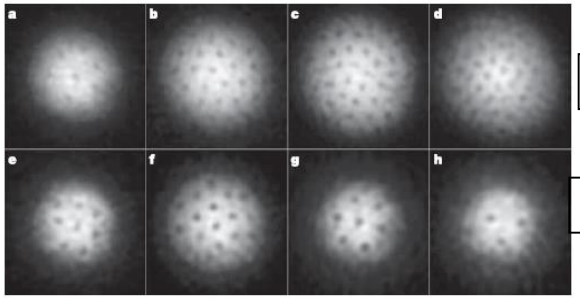

bosons

fermions

Experiments with ultracold Li6 atoms: pictures of the vortex lattice.

Figure 2 | Vortices in a strongly interacting gas of fermionic atoms on the BEC- and the BCS-side of the Feshbach resonance. At the given field, the cloud of lithium atoms was stirred for 300 ms (**a**) or 500 ms (**b**–**h**) followed by an equilibration time of 500 ms. After 2 ms of ballistic expansion, the magnetic field was ramped to 735 G for imaging (see text for details). The magnetic fields were 740 G (**a**), 766 G (**b**), 792 G (**c**), 812 G (**d**), 833 G (**e**), 843 G (**f**), 853 G (**g**) and 863 G (**h**). The field of view of each image is 880 μm × 880 μm.

M.W. Zwierlein *et al.*, Nature, 435, 1047 (2005)

The well known effects in superconductors where the simplified BCS approach fails

1) Quantum vortices, solitonic excitations related to pairing field (e.g. domain walls)

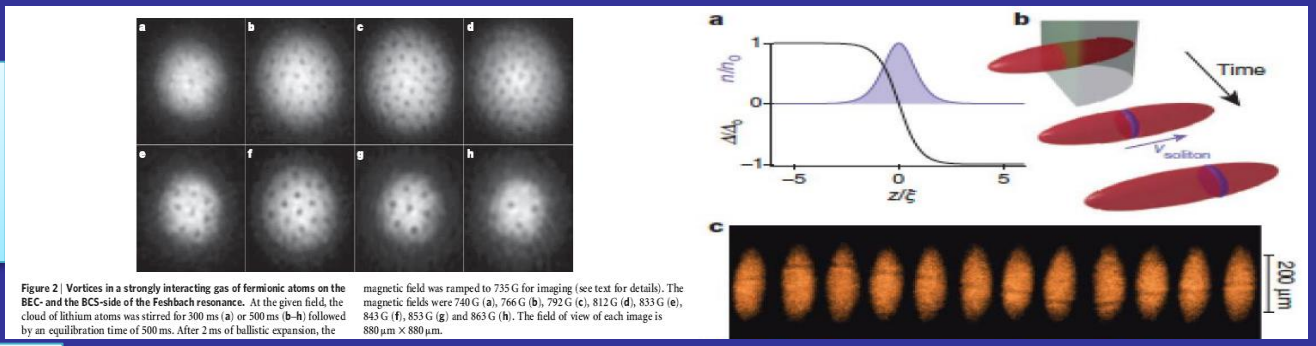

Figure 2 | Vortices in a strongly interacting gas of fermionic atoms on the BEC- and the BCS-side of the Feshbach resonance. At the given field, the cloud of lithium atoms was stirred for 300 ms (**a**) or 500 ms (**b**–**h**) followed by an equilibration time of 500 ms. After 2 ms of ballistic expansion, the magnetic field was ramped to 735 G for imaging (see text for details). The magnetic fields were 740 G (**a**), 766 G (**b**), 792 G (**c**), 812 G (**d**), 833 G (**e**), 843 G (**f**), 853 G (**g**) and 863 G (**h**). The field of view of each image is 880 μm × 880 μm.

2) Bogoliubov – Anderson phonons

3) proximity effects: variations of the pairing field on the length scale of the coherence length.

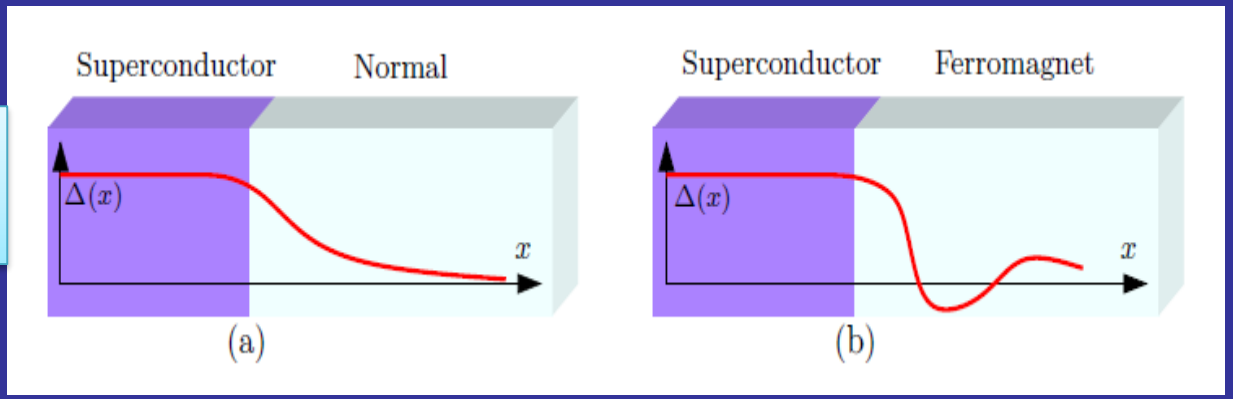

4) physics of Josephson junction (superfluid - normal metal), pi-Josephson junction (superfluid - ferromagnet)

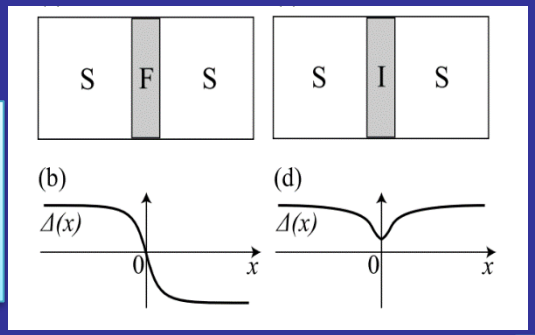

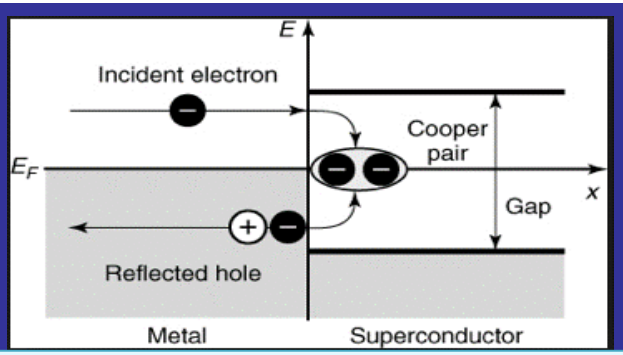

5) Andreev reflection (particle-into-hole and hole-into-particle scattering) Andreev states cannot be obtained within BCS

Pairing correlations in DFT

One may extend DFT to superfluid systems by defining the pairing field:

$$\Delta(\mathbf{r}\sigma,\mathbf{r}'\sigma') = -\frac{\delta E(\rho,\chi)}{\delta\chi^*(\mathbf{r}\sigma,\mathbf{r}'\sigma')}.$$

L. N. Oliveira, E. K. U. Gross, and W. Kohn, Phys. Rev. Lett. 60 2430 (1988).

O.-J. Wacker, R. Kümmel, E.K.U. Gross, Phys. Rev. Lett. 73, 2915 (1994).

Triggered by discovery of high-Tc superconductors

and introducing anomalous density $\chi(\mathbf{r}\sigma,\mathbf{r}'\sigma') = \langle\hat{\psi}_{\sigma'}(\mathbf{r}')\hat{\psi}_{\sigma}(\mathbf{r})\rangle$

However in the limit of the local field these quantities diverge unless one renormalizes the coupling constant:

$$\begin{aligned}\Delta(\mathbf{r}) &= g_{eff}(\mathbf{r})\chi_c(\mathbf{r})\\ \frac{1}{g_{eff}(\mathbf{r})} &= \frac{1}{g(\mathbf{r})} - \frac{mk_c(\mathbf{r})}{2\pi^2\hbar^2}\left(1 - \frac{k_F(\mathbf{r})}{2k_c(\mathbf{r})}\ln\frac{k_c(\mathbf{r})+k_F(\mathbf{r})}{k_c(\mathbf{r})-k_F(\mathbf{r})}\right)\end{aligned}$$

which ensures that the term involving the kinetic and the pairing energy density is finite:

$$\frac{\tau_c(r)}{2m} - \Delta(r)\chi_c(r), \qquad \tau_c(r) = \nabla\cdot\nabla'\rho_c(r,r')\big|_{r=r'}$$

A. Bulgac, Y. Yu, Phys. Rev. Lett. 88 (2002) 042504

A. Bulgac, Phys. Rev. C65 (2002) 051305

It allows to reduce the size of the problem for static calculations by introducing the energy cutoff

TDDFT equations with local pairing field (TDSLDA):

$$i\hbar\frac{\partial}{\partial t}\begin{pmatrix} u_{k\uparrow}(\mathbf{r},t) \\ u_{k\downarrow}(\mathbf{r},t) \\ v_{k\uparrow}(\mathbf{r},t) \\ v_{k\downarrow}(\mathbf{r},t) \end{pmatrix} = \begin{pmatrix} h_{\uparrow,\uparrow}(\mathbf{r},t) & h_{\uparrow,\downarrow}(\mathbf{r},t) & 0 & \Delta(\mathbf{r},t) \\ h_{\downarrow,\uparrow}(\mathbf{r},t) & h_{\downarrow,\downarrow}(\mathbf{r},t) & -\Delta(\mathbf{r},t) & 0 \\ 0 & -\Delta^*(\mathbf{r},t) & -h^*_{\uparrow,\uparrow}(\mathbf{r},t) & -h^*_{\uparrow,\downarrow}(\mathbf{r},t) \\ \Delta^*(\mathbf{r},t) & 0 & -h^*_{\uparrow,\downarrow}(\mathbf{r},t) & -h^*_{\downarrow,\downarrow}(\mathbf{r},t) \end{pmatrix} \begin{pmatrix} u_{k\uparrow}(\mathbf{r},t) \\ u_{k\downarrow}(\mathbf{r},t) \\ v_{k\uparrow}(\mathbf{r},t) \\ v_{k\downarrow}(\mathbf{r},t) \end{pmatrix}$$

The form of $h(r,t)$ and $\Delta(r,t)$ is determined by EDF (Energy Density Functional)

- **The system is placed on a large 3D spatial lattice.**
- **No symmetry restrictions.**
- **Number of PDEs is of the order of the number of spatial lattice points.**

Table 1: Comparison of profit gained by using GPUs instead of CPUs for two example lattices. The timing was obtained on Titan supercomputer. Note, Titan has 16x more CPUs than GPUs.

		CPU implementation		GPU implementation		
$N_xN_yN_z$	Number of HFB equations	# of CPUs	time per step	# of GPUs	time per step	***SPEEDUP***
48^3	110,592	110,592	3.9 sec	6,912	0.39 sec	**10**
64^3	262,144	262,144	20 sec	16,384	0.80 sec	**25**

The main advantage of TDSLDA over TDHF (+TDBCS) is related to the fact that in TDSLDA the pairing correlations are described as a true complex field which has its own modes of excitations, which include spatial variations of both amplitude and phase. Therefore in TDSLDA description the evolution of nucleon Cooper pairs is treated consistently with other one-body degrees of freedom.